Available online at www.sciencedirect.com
ScienceDirect
Journal of the European Ceramic Society 30 (2010) 73–79
www.elsevier.com/locate/jeurceramsoc

Nanoindentation of melt-extracted amorphous YAG and YAG:Eu, Nd micrometric fibers synthesized by the citrate precursor method

R. López [a], E.A. Aguilar [a,*], J. Zárate-Medina [a], J. Muñoz-Saldaña [b,c], D. Lozano-Mandujano [b]

[a] *Instituto de Investigaciones Metalúrgicas, UMSNH, Edificio "U", C.U., Morelia, Michoacán, CP 58060, Mexico*
[b] *Centro de Investigación y Estudios Avanzados del IPN. Unidad Querétaro, Libramiento Norponiente No. 2000, Fracc. Real de Juriquilla, Querétaro, Qro., CP 76230, Mexico*
[c] *Centro de Investigación en Materiales Avanzados y Laboratorio Nacional de Nanotecnología-Chihuahua. Miguel de Cervantes 120, Complejo Industrial Chihuahua, Chihuahua, 31109 Mexico*

Received 8 April 2009; received in revised form 21 July 2009; accepted 27 July 2009
Available online 2 September 2009

Abstract

We report the structural and mechanical characterization of yttrium aluminum garnet fibers obtained with Eu and Nd additions by the melt-extraction method (ME). Powders were synthesized by the modified citrate precursor method. This method produces in a single step of heat treatment the pure YAG phase avoiding the formation of $YAlO_3$, $Y_4Al_2O_9$ or Y_2O_3 phases. Rare earth additions delay proportionally to the added quantity of dopant the crystallization temperature of the YAG phase. Using crystalline powders, cylindrical fibers (20–30 μm) in an amorphous state irrespective of doping type and amount were obtained by ME. Nanoindentation tests were carried out showing hardness and reduced elastic modulus of 5.8 ± 0.3 and 79.3 ± 4.9 GPa for pure YAG fibers, respectively. 2 at.% additions of Nd to the YAG phase lead to an increment in hardness and reduced elastic modulus (9.1 and 128.6 GPa, respectively). However, further increments of Eu or Nd (5 at.%) cause a clear degradation of the mechanical properties respective to the values reached with 2 at.% of rare earth additions. This degradation effect seems to be correlated to the atomic interaction due to difference between radii of Eu and Nd, respective to Y.

Keywords: Fibres; Hardness; Electron microscopy; Sol–gel processes; Melt extraction; YAG

1. Introduction

Yttrium Aluminum Garnet (YAG) has a cubic structure that belongs to spatial group *Ia3d* with a lattice parameter of 12.01 Å, where metallic ions occupy *d*, *a* and *c* positions (tetrahedral, octahedral and dodecahedral sites, respectively). The aluminum atoms occupy 24 *d* sites and 16 *a* sites and yttrium is typically reported in 24 *c* sites.[1] This compound has several applications, either as pure phase or doped with elements such as Nd^{3+}, Eu^{3+}, Tb^{3+}, Cr^{3+} and Ce^{3+} in laser systems production, coating of electronic devices, including the phosphor for cathode ray tubes.[2–6] Recently, this compound has been considered as a good material for structural applications at high temperatures[7,8] and as ceramic matrix reinforcement. These applications are intimately related to the optical properties, chemical stability at high temperatures, excellent corrosion resistance and good mechanical properties.

There are several methods reported in the literature for the synthesis of YAG powders. The conventional solid state reaction method of powders[9] for the synthesis of YAG requires high temperatures (1600 °C) and a prolonged time of calcination. Several wet methods of synthesis have been developed[10–16] to diminish the crystallization temperature and increase the purity of the resulting YAG materials. The presence of intermediate phases such as metastable $YAlO_3$, $Y_4A_2O_9$ and Y_2O_3 has been observed in several synthesis methods.[13,14] Recently, Li et al.[7] reduced considerably the temperature of crystallization, obtaining the YAG crystalline phase approximately at 300 °C for 2 h, using a pressurized reactor (pressures above 10 MPa) to achieve the reaction.

Different methods to prepare doped- and undoped-YAG and Al_2O_3–Y_2O_3 fibers have been also reported in the literature such as sol–gel,[17,18] melt growth techniques such as micro-pulling-down (μ-PD) method[19–21] and the internal crys-

* Corresponding author. Tel.: +52 443 3223500x4008; fax: +52 443 3223500x4010.
E-mail address: aareyes@umich.mx (E.A. Aguilar).

0955-2219/$ – see front matter © 2009 Elsevier Ltd. All rights reserved.
doi:10.1016/j.jeurceramsoc.2009.07.028

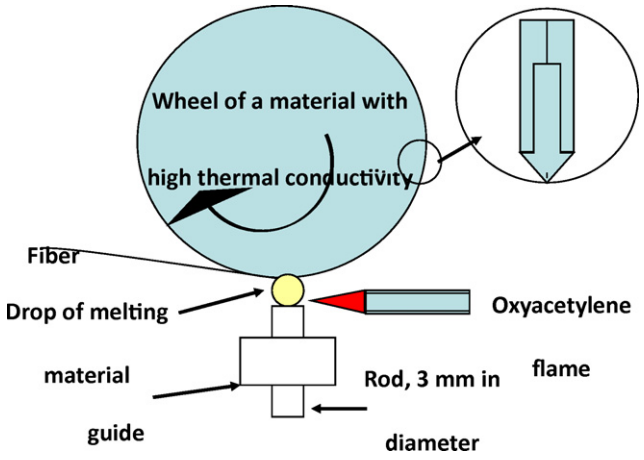

Fig. 1. Schematic representation of the used melt-extraction method for the preparation of YAG fibers.

tallization method,[22,23] the levitation technique,[24] and melt extraction.[25,26] The melt-extraction method was developed initially by Maringer and Mobley[27] in 1974. Originally, it was developed to obtain metallic fibers mainly of steel and certain alloys to reinforce concrete and ceramic materials. Some modifications to obtain fibers of ceramics such as $CaO–Al_2O_3$, $Al_2O_3–ZrO_2$, $Al_2O_3–ZrO_2–SiO_2$ and $Al_2O_3–ZrO_2–TiO_2$[28–30] were made on the process, and more recently fibers of YAG and some compositions of the system $Al_2O_3–Y_2O_3$ have been produced.[25,26]

Reinforcement of ceramics by adding micrometric YAG fibers seems to have great potential to produce high performance structural ceramic composites. Measurement of the mechanical properties of fiber cross-sections provides information to demonstrate the effectiveness of reinforcement. Depth sensing indentation is the most suitable method to characterize the mechanical impact of the fibers at the micrometric and nanometric scale.

In this work the melt-extraction technique was used to obtain amorphous fibers with the YAG composition, previously synthesized by the modified citrate precursor method with additions of Nd_2O_3 and Eu_2O_3. The prepared fibers were mechanically evaluated "as extracted" and as a function of the composition by nanoindentation. Depth sensing indentation in the Hysitron Ubi1 system is applied specifically to determine hardness and reduced elastic modulus by analyzing the load–depth curves.

2. Experimental

Aluminum nitrate (99.9% J.T. Baker), yttrium nitrate (99.9% Aldrich), europium oxide, neodymium oxide (99.99% Alpha-Aesar), citric acid (J.T. Baker), ethylenglycol (99.9% J.T. Baker) and deionized water were used as raw materials.

Solutions with compositions corresponding to YAG, YAG:2 at.% Eu and YAG:5 at.% Eu as well as YAG:2 at.% Nd and YAG:5 at.% Nd were prepared by the citrate precursor method as reported elsewhere.[6] The Eu and Nd additions in at.% were referred to the yttrium content in the garnet. These solutions were fed separately into a spray dryer (Mini Spray-Dryer, ADL-

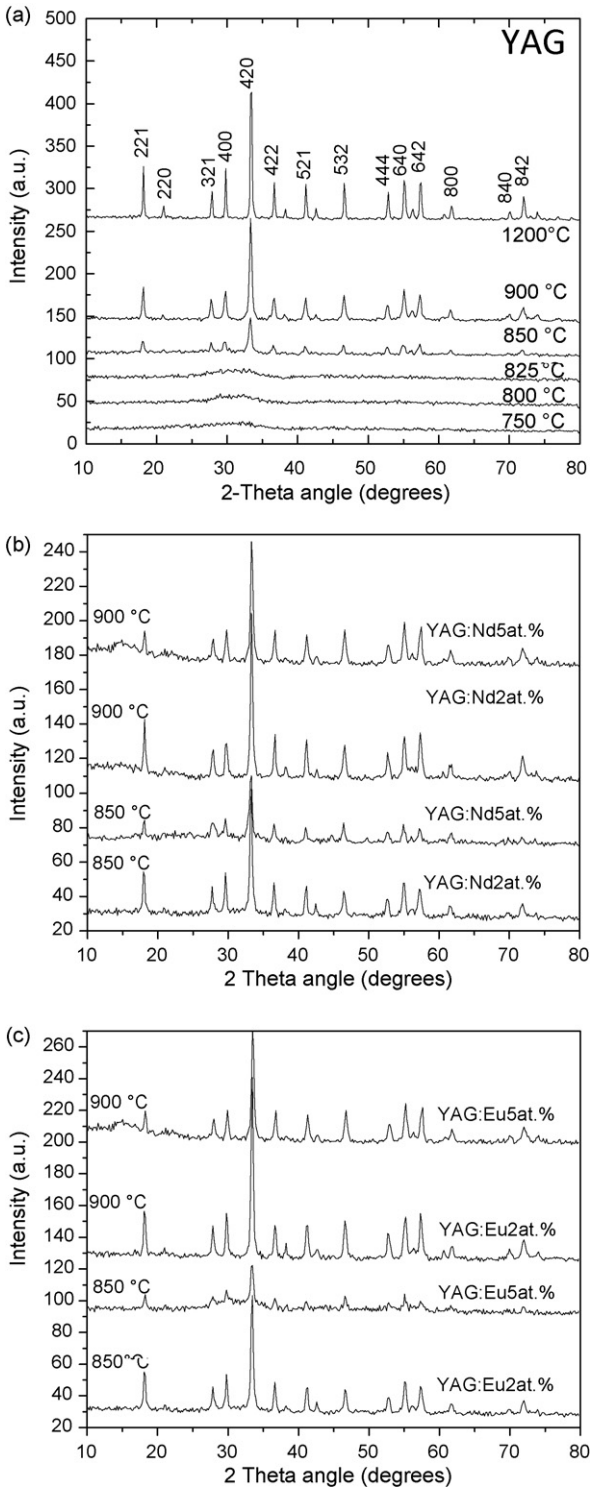

Fig. 2. XRD patterns of (a) pure YAG powders at different calcinations temperatures and (b) and (c) doped YAG powders with 2 and 5 at.% of Nd and Eu, respectively, calcined at 850 and 900 °C.

31) to eliminate the solvent and to produce precursor powders. These powders were thereafter calcined from 750 to 1200 °C to promote the crystallization of the YAG phase. Heat treated powder samples were characterized by X-ray diffraction using a SIEMENS D5000 diffractometer with Cu Kα radiation operated at 20 kV. Several micrographs of the samples were obtained

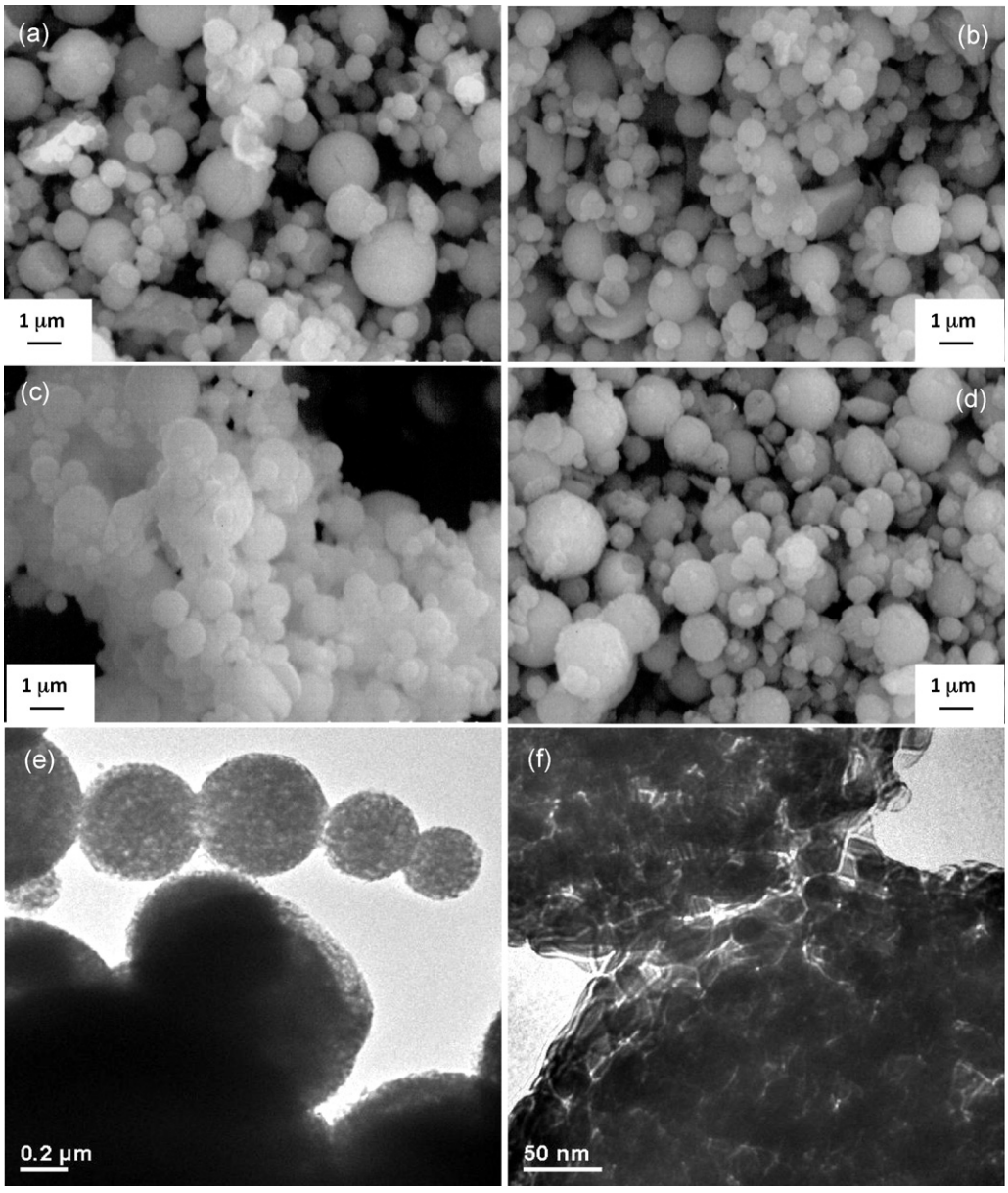

Fig. 3. Typical SEM a micrograph of YAG powders processed by spray drying: (a) YAG:2 at.% Eu, (b) YAG:5 at.% Eu, (c) YAG:2 at.% Nd and (d) YAG:5 at.% Nd. High resolution TEM images of undoped YAG fibers showing (e) several spherical shaped agglomerates and (f) close up view of the contact zone between two agglomerates showing the interaction between single YAG particles.

by scanning electron microscopy (SEM, JEOL JSM-6400) to estimate the characteristics of agglomerates as well as by transmission electron microscopy (TEM, Phillips TECNAI super Twin) with an acceleration voltage of 200 kV to measure the particle size and representative unit cell parameters. For the extraction of fibers from the melt, preforms were prepared using the synthesized powders. Spray dried crystalline powders also calcined at 900 °C were mixed with 5 wt.% of hydroxypropyl-cellulose as plasticizer and distilled water. All mixtures were extruded to obtain cylindrical rods with 3 mm diameter and 12 cm length. The prepared rods were dried in air for 24 h at room temperature followed by calcination at 1000 °C for 30 min to eliminate the water and hydroxypropyl-cellulose. Finally the rods were sintered at 1500 °C for 1 h to acquire sufficient resistance for later handling. Fibers were prepared by melt extraction using a copper–beryllium wheel (alloy C17 500) of 14 cm diameter as schematically shown in Fig. 1. Copper was chosen because of its good thermal conductivity necessary to extract the heat from the liquid and to promote rapid solidification. The speed-controlled wheel has an edge of 8 μm in thickness; the speed feeding of the ceramic rod was also controlled to be 3 mm/min. The sintered rod was melted using an oxy-acetylene torch to form a small molten drop just in the top and beneath the rotating wheel. The shallow contact of the wheel tip with the molten drop resulted in the extraction and rapid solidification of the fibers. Under these conditions, the fiber extraction tangential speed was 1.5 m/s. Characterization of fibers was done by X-ray diffraction (SIEMENS D5000) to identify crystalline phases and

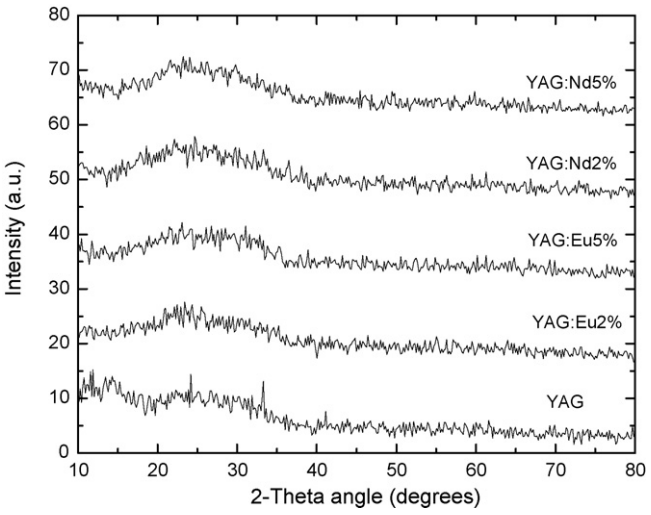

Fig. 4. XRD patterns of "as extracted" pure and doped YAG amorphous fibers.

scanning electron microscopy (SEM JEOL 6400) to observe the dimensions, morphology, and surface conditions of fibers. A Hysitron Ubi1 nanoindentation system with a Berkovich diamond tip (tip radius of 830 μm) in the load range of 50 μN to 9 mN was used to determine the hardness and reduced elastic modulus of fiber transverse cross-sections. To do this, several fibers were mounted in a polymer matrix to polish their transverse cross-section with alumina suspensions with particle size in the range of 3 and 0.03 μm and a final polishing step with commercial colloidal silica suspension (Mastermet II, Buehler). Indentation imprints in a "load control" mode of force versus time were carried out at different maximal loads covering most of the fiber cross-section.

3. Results and discussion

Fig. 2a shows typical XRD patterns of pure YAG powders produced by the modified citrate precursor method and thermally treated at 750, 800, 825, 850, 900 and 1200 °C. YAG powders with additions of 2 and 5% of neodymium and europium heat treated at 850 and 900 °C are shown in the same figure (Fig. 2b and c). In all cases, calcination temperatures below 850 °C lead to powders in an amorphous state. Powder crystallization to YAG phase occurs above 850 °C, irrespective of the europium or neodymium content and without the formation of Y–Al–O intermediate phases. The crystalline phase, as observed in the diffraction patterns at temperatures above 850 °C, corresponds to YAG according to the JCPDS card 33-0040. Additions of rare earths seem to delay the crystallization of the YAG phase as observed in the lower intensity of the diffraction peaks. This behavior seems to be proportional to the dopant quantity. For instance, samples prepared with 2 at.% showed higher intensity than those with 5 at.% of europium or neodymium in all the diffracted planes. Considering that the Eu enters in solid solution in YAG, occupying dodecahedral sites, that are originally occupied by Y ions and that the covalent radii of Y, Nd and Eu are 1.62, 1.64 and 1.85 Å, respectively, one can expect that europium ions would need a longer time for diffusion than yttrium ions, slowing re-arrangement. This effect can be observed by comparing XRD patterns of doped YAG at 850 °C (Fig. 2b and c) where a major decrease in intensity of the diffraction peaks is obtained with 5 at.% of europium. Thus, this behavior suggests that at higher Eu or Nd dopant concentrations, the YAG crystallization is delayed.

Typical SEM images of powders with additions of 2 and 5% of europium and neodymium both calcined at 900 °C for

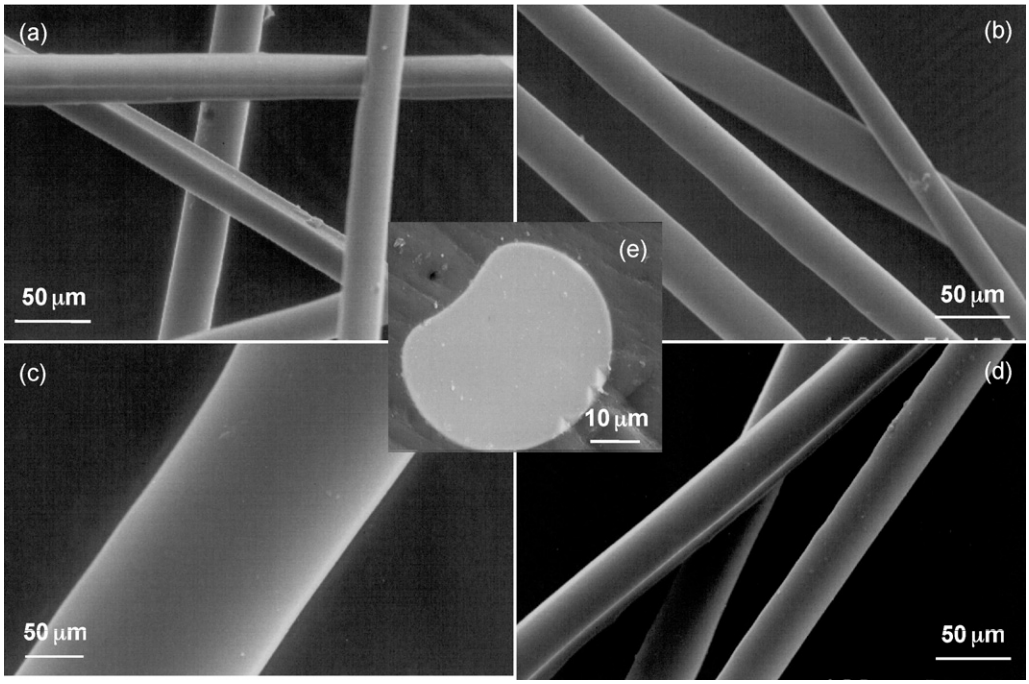

Fig. 5. SEM images showing the outer surface appearance of "as extracted" (a) undoped YAG, (b) YAG:Nd2 at.%, (c) YAG:Eu2 at.% and (d) YAG:Eu5 at.% amorphous fibers. The micrograph of (e) corresponds to a transverse cross-section of the undoped YAG fiber.

1 h are shown in Fig. 3. Size quantification of the spherical agglomerates by image analysis of these micrographs revealed an average diameter of 0.86 ± 0.45 μm. Spherical morphology is characteristic of agglomerates obtained by spray drying.[6] Neither morphology nor size of the spherical agglomerates seems to be influenced by the composition of the feed solution or by the heat treatment at temperatures as high as 1200 °C. The spray drying method produces agglomerates of controlled size, which is an important advantage compare with other methods.[1,10] An advantage of spherical agglomerates is their excellent fluidity, which is beneficial for the elaboration of pressed bodies. In the same Fig. 3, typical high resolution transmission electron microscopy micrographs of undoped YAG powder clearly show that such dried spherical agglomerates are composed of several equiaxially shaped particles with a diameter of 25 ± 4 nm. Again, these results are very similar to the powder samples prepared with rare earth additions.

After fiber preparation by using the melt-extraction method, all samples were again characterized by XRD and the results are shown in Fig. 4. These diffraction patterns reveal an amorphous state of all the prepared systems, irrespective of the dopant type and content. This behavior is related to the high cooling rates involved during the melt-extraction process (typically in the order of 10^5 K s^{-1}).

Morphology of the fibers can be observed in the SEM micrographs of Fig. 5 for pure YAG (a) and YAG:Nd2 at.% (b), YAG:Eu2 at.% (c) and YAG:Eu5 at.%. All fibers showed smooth surfaces and semi-circular transverse cross-sections except for a mark of the copper–beryllium wheel through the length of the fibers, formed during fiber extraction. The inset of the same figure (e) shows the transverse cross-section of a typical pure YAG fiber mounted in a polymer matrix and polished according to the method described earlier. All fibers showed diameters in the range of 20–30 μm mainly influenced by the operation conditions during the melt extraction described in Section 2, and irrespective of the dopant type and quantity.

As mentioned before, all fibers were tested by nanoindentation with the load control mode using variable loads consistently on the fiber transverse cross-section. Fig. 6 shows typical contact mode AFM micrographs of the YAG:Nd5 at.% fiber, showing nanoindentation imprints on the polished fiber surface. Polishing with a commercial colloidal silica suspension produced surface quality of the fiber cross-section with an average roughness close to 3 nm, giving rise to the best surface conditions for nanoindentation testing. Indentations are well distributed along the surface, where hardness and elastic modulus were determined by the Oliver and Pharr method.[31] Indentations at high loads are located near the fiber border, whereas the low loads are most of them well in the middle of the fiber cross-section. Indentation imprints were repeatedly located in this way, which allowed us to evaluate the existence of any differences in hardness and elastic modulus from the border to the center of the fiber.

Typical indentation results for the YAG:Nd2 at.% fiber are shown in Fig. 7 (load–penetration depth curves and hardness and reduced elastic modulus as a function of contact penetration depth). There was practically no variation of hardness between the edge and the center of the fiber, as can be seen from the horizontal line from Fig. 7(b). For the case of reduced elastic modulus, there is a surface effect of higher values with respect to higher penetration depths changing from around 120 to 130 GPa, respectively for this fiber. This effect is probably due to the residual stresses induced in the fibers during the polishing procedures. There is, however a clear influence of the doping type and amount on the mechanical properties of fibers. A comparison of load against penetration depth curves of undoped and Nd and Eu-doped fibers, all of them "as extracted" are shown in Fig. 8. There, clearly different behaviors are observed when indenting the different prepared fibers. Quantification of hardness and reduced elastic modulus values are summarized in Table 1.

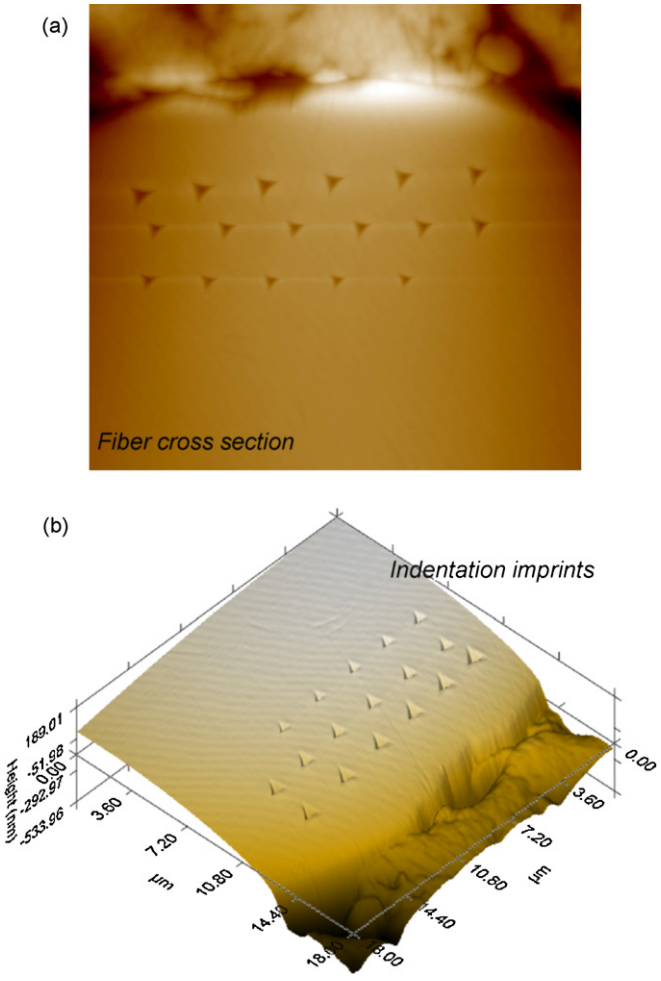

Fig. 6. AFM micrographs in contact mode of a YAG:Nd5 at.% fiber cross-section showing typical nanoindentation marks carried out at variable load in the "load control mode".

Table 1
Hardness and elastic modulus results of the prepared YAG fibers.

Sample	Hardness (GPa)	Reduced elastic modulus (GPa)
YAG	5.8 ± 0.3	79.3 ± 4.9
YAG:Eu2 at.%	6.3 ± 0.5	96.9 ± 3.9
YAG:Eu5 at.%	4.9 ± 0.1	61.9 ± 6.2
YAG:Nd2 at.%	9.1 ± 0.1	128.6 ± 3.1
YAG:Nd5 at.%	7.8 ± 0.1	68.1 ± 1.6

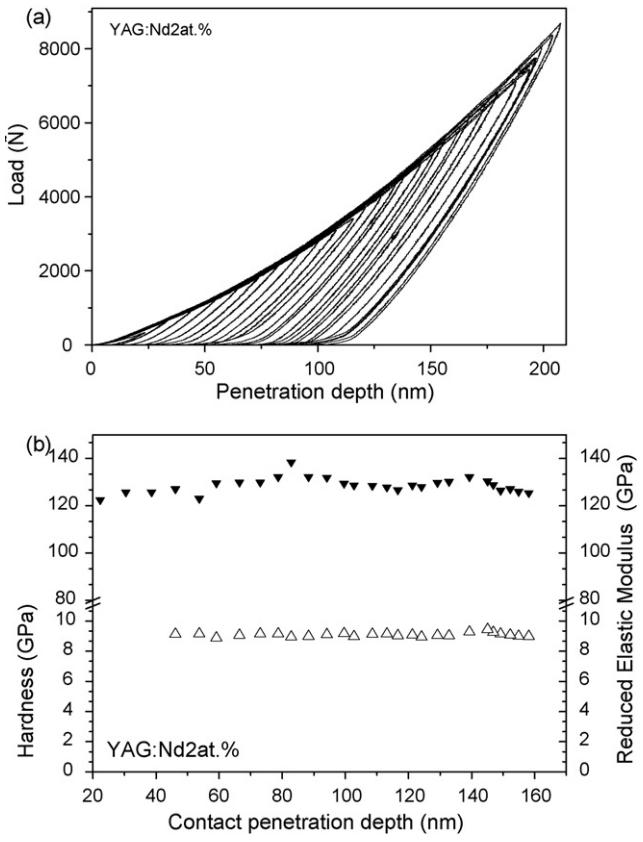

Fig. 7. Typical load–penetration curves as well as the results of hardness and reduced elastic modulus as a function of penetration depth of a YAG:Nd2 at.% amorphous fiber obtained by the "load control" mode in nanoindentation.

Rare earths additions of 2 at.% clearly enhance the hardness and elastic modulus of the fibers. For instance, 2 at.% additions of Nd increase hardness and reduced elastic modulus from 5.8 ± 0.3 and 79.3 ± 4.9 GPa of the undoped YAG fiber to 9.1 ± 0.1 and 128.6 ± 3.1 GPa, respectively, which are the highest effect reached in doped YAG fibers. Further increments of the rare earths (5 at.% Eu or Nd) reduce dramatically the mechanical performance. The lowest values were obtained for YAG:Eu5 at.% fibers.

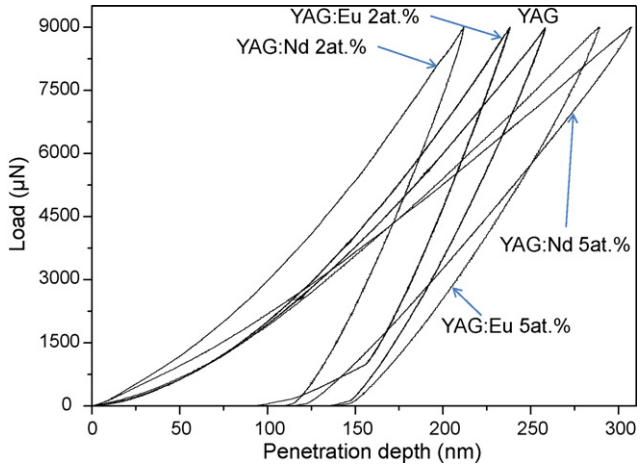

Fig. 8. Comparison of the load–penetration depth curves at high loads of undoped YAG with the corresponding data of 2 and 5 at.% of Eu and Nd doped YAG fibers.

It has been reported by Weber et al.[24] that there are at least two phenomena that may affect the fiber-pulling behavior observed for pure YAG and doped compositions, which in turn affect their mechanical behavior. The first in the greater sensitivity of undercooling behavior in general for the pure composition. It is well known that YAG crystal growth can encounter difficulties due to crystallization of other phases. Evidently, undercooled pure YAG melts are sensitive to small compositional or other differences associated with preheating, and this sensitivity may also influence the glass-fiber-pulling process.

The second phenomenon that may affect fiber-pulling was reported by Aasland and McMillan (as referred by Weber et al.[24]). They found that a mixture of two glasses forms on rapid cooling of Al_2O_3–Y_2O_3 melts containing 24–32 mol% Y_2O_3. The difficulty in making pure YAG fibers and the ease with which doped fibers were formed may result for different melt-transition kinetics for the pure and doped materials.

4. Conclusion

Homogeneous amorphous fibers of 20–30 μm in diameter have been successfully produced by the melt-extraction method using crystalline YAG powders prepared by the modified citrate precursor method. This method allowed a crystallization temperature of the YAG phase in the powders of 850 °C and homogeneous doping with Nd and Eu up to 5 at.% avoiding formation of other Y–Al–O phases, different to the Y–Al garnet structure. This behavior is attributed to the high homogeneity of the elements in the spray dried precursory powders. The melt-extraction method of rods prepared with powders calcined at 900 °C allowed the preparation of fibers in an amorphous state due to the high cooling rates of the melt. Fibers with additions of 2 at.% of both Eu or Nd showed an increase in hardness and reduced elastic modulus (9.1 ± 0.1 and 128.6 ± 3.1 GPa) with respect to pure YAG amorphous fibers (5.8 ± 0.3 and 79.3 ± 4.9 GPa). Additions of 5 at.% of Eu or Nd diminished the mechanical properties. Here, the ionic radii difference, particularly between Y and Eu seems to affect the chemical binding behavior of the atoms in the composition of YAG fibers, which determines their poor mechanical properties.

Acknowledgments

The authors want to acknowledge CONACYT-Mexico for financial support.

References

[1]. Brown, K. R. and Bonnell, D. A., Segregation in yttrium aluminum garnet. II. Theoretical calculations. *J. Am. Ceram. Soc.*, 1999, **82**, 2431–2441.

[2]. Fu, Y.-P., Tsao, S. and Hu, C.-Ti, Preparation of $Y_3Al_5O_{12}$:Cr powders by microwave-induced combustion process and their luminescent properties. *J. Alloys Compd.*, 2005, **395**, 227–230.

[3]. Fu, Y.-P., Wen, S.-B. and Hsu, C.-S., Preparation and characterization of $Y_3Al_5O_{12}$:Ce and Y_2O_3:Eu phosphors powders by combustion process. *J. Alloys Compd.*, 2008, **458**, 318–322.

[4]. Jia, D., Wang, Y., Guo, X., Li, K., Zou, Y. K. and Jia, W., Synthesis and characterization of YAG:Ce^{3+} LED nanophosphors. *J. Electrochem. Soc.*, 2007, **154**, J1–J4.

[5]. Na, Z., Dajian, W., Lan, L., Yanshuang, M., Xiaosong, Z. and Nan, M., YAG:Ce phosphors for WLED via nano-pseudoboehmite sol–gel route. *J. Rare Earths*, 2006, **24**, 294–297.

[6]. Pan, Y., Wu, M. and Su, Q., Comparative investigation on synthesis and photoluminiscence of YAG:Ce phosphor. *Mater. Sci. Eng. B*, 2004, **106**, 251–256.

[7]. Li, X., Liu, H., Wang, J., Cui, H., Zhang, X. and Han, F., Preparation of YAG:Nd nano-sized powder by co-precipitation method. *Mater. Sci. Eng. A*, 2004, **379**, 347–350.

[8]. Sun, Z., Yuan, D., Li, H., Duan, X., Wei, X., Xu, H. and Luan, C., Synthesis of yttrium aluminum garnet (YAG) by a new sol–gel method. *J. Alloys Compd.*, 2004, **379**, L1–L3.

[9]. Ikesue, A., Furusato, I. and Kamata, K., Fabrication of polycrystalline, transparent YAG ceramics by a solid-state reaction method. *J. Am. Ceram. Soc.*, 1995, **78**, 225–228.

[10]. Zárate, J., López, R. and Aguilar, E. A., Synthesis of yttrium aluminum garnet by modifying the citrate precursor method. *Adv. Tech. Mat. Mat. Proc.*, 2005, **7**, 53–56.

[11]. Liu, Y. and Gao, L., Low-temperature synthesis of nanocrystalline yttrium aluminum garnet powder using triethanolamine. *J. Am. Ceram. Soc.*, 2003, **86**, 1651–1653.

[12]. Lu, Q., Dong, W., Wang, H. and Wang, X., A novel way to synthesize yttrium aluminum garnet from metal–inorganic precursors. *J. Am. Ceram. Soc.*, 2002, **85**, 490–492.

[13]. Han, K. R., Koo, H. J. and Lim, C. S., A simple way to synthesize yttrium aluminum garnet by dissolving yttria powder in alumina sol. *J. Am. Ceram. Soc.*, 1999, **82**, 1598–1600.

[14]. Hassanzadeh-Tabrizi, S. A., Taheri-Nassaj, E. and Sarpoolaky, H., Synthesis of an alumina-YAG nanopowder via sol–gel method. *J. Alloys Compd.*, 2008, **456**, 282–285.

[15]. Cinibulk, M. K., Synthesis of yttrium aluminum garnet from a mixed-metal citrate precursor. *J. Am. Ceram. Soc.*, 2000, **83**, 1276–1278.

[16]. Jung, H.-G., Cheong, Y.-H., Han, I.-D., Kim, S.-J. and Kang, S.-G., Low-temperature fabrication of polycrystalline yttrium aluminum garnet powder via a mechanochemical solid reaction of nanocrystalline yttria with transition alumina. *Solid State Phenomena*, 2003, **135**, 7–10.

[17]. Shojaie-Bahaabad, M., Taheri-Nassaj, E. and Naghizadeh, R., Effect of yttria on crystallization and microstructure of an alumina-YAG fiber prepared by aqueous sol–gel process. *Ceram. Int.*, 2009, **35**, 391–396.

[18]. Towata, A., Hwang, H. J., Yasuoka, M., Sando, M. and Niihara, K., Preparation of polycrystalline YAG/alumina composite fibers and YAG fiber by sol–gel method. *Composites A*, 2001, **32**, 1127–1131.

[19]. Lee, J. H., Yoshikawa, A., Fukuda, T. and Waku, Y., Growth and characterization of $Al_2O_3/Y_3Al_5O_{12}/ZrO_2$ ternary eutectic fibers. *J. Cryst. Growth*, 2001, **231**, 115–120.

[20]. Lee, J. H., Yoshikawa, A., Kaiden, H., Lebbou, K., Fukuda, T., Yoon, D. H. and Waku, Y., Microstructure of Y_2O_3 doped Al_2O_3/ZrO_2 eutectic fibers grown by the micro-pulling-down method. *J. Cryst. Growth*, 2001, **231**, 179–185.

[21]. Cornacchia, F., Alshourbagy, M., Toncelli, A., Tonelli, M., Ogino, H., Yoshikawa, A. and Fukuda, T., Growth and spectroscopic properties of Er:YAG crystalline fibers. *J. Cryst. Growth*, 2005, **275**, 534–540.

[22]. Kurlov, V. N., Kolchin, A. A., Dodonov, A. M., Shmurak, S. Z., Strukova, G. K. and Shmyt'ko, I. M., Growth of YAG:Re^{3+} (Re = Ce, Tb, Eu) fibers for imaging systems. *Nucl. Instrum. Methods Phys. Res. Sect. A*, 2005, **537**, 219–222.

[23]. Mileiko, S. T., Kurlov, V. N., Kolchin, A. A. and Kiiko, V. M., Fabrication properties and usage of single-crystalline YAG fibres. *J. Eur. Ceram. Soc.*, 2002, **22**, 1831–1837.

[24]. Weber, J. K. R., Felten, J. J., Cho, B. and Nordine, P. C., Glass fibers of pure and erbium or neodymium-doped yttria alumina compositions. *Nature*, 1998, **393**, 769–771.

[25]. Aguilar, E. A., Drew, R. A. L., Saruhan, B., Milz, C. and Hildman, B., Processing and crystallization of rapidly solidified Al_2O_3–Y_2O_3 fibres. *Br. Ceram. Trans.*, 2000, **6**, 256–259.

[26]. Aguilar, E. A. and Drew, R. A. L., Melt extraction processing of structural Y_2O_3–Al_2O_3 fibers. *J. Eur. Ceram. Soc.*, 2000, **20**, 1091–1098.

[27]. Stewart, O. M., Maringer, R. E. and Mobley, C. E., Method of producing continuous filaments using a rotating heat-extracting member. U.S. Patent 3812901, 28 May 1974.

[28]. Allahverdi, M., Drew, A. R. L. and Ström-Olsen, J. O., Melt-extracted oxide ceramics fibres—the fundamentals. *J. Mater. Sci.*, 1996, **31**, 1035–1042.

[29]. Ström-Olsen, J. O., Rudkowska, G. and Rudkowski, P., Fine metallic and ceramic fibers by melt extraction. *Mater. Sci. Eng. A*, 1994, **179/180**, 158–162.

[30]. Allahverdi, M., Drew, R. A. L., Rudkowska, P., Rudkowski, G. and Ström-Olsen, J. O., Amorphous $CaO.Al_2O_3$ fibers by melt extraction. *Mater. Sci. Eng. A*, 1996, **207**, 12–21.

[31]. Oliver, W. C. and Pharr, G. M., A new improved technique for determining hardness and elastic modulus using load and sensing indentation experiments. *J. Mater. Res.*, 1992, **7**, 1564–1582.